CIRP Journal of Manufacturing Science and Technology 55 (2024) 88–97

Contents lists available at ScienceDirect

CIRP Journal of Manufacturing Science and Technology

journal homepage: www.elsevier.com/locate/cirpj

Investigation of the effects of CO_2 pre-cooling on the cooling capacity for cryogenic cooling in machining operations

Trixi Meier *, Jan Harald Selzam, Andreas Röckelein, Nico Hanenkamp

University Erlangen-Nuremberg, Institute for Resource and Energy Efficient Production Systems (REP), Dr.-Mack-Str. 81, Fürth 90762, Germany

ARTICLE INFO

Keywords:
Cryogenic minimum quantity lubrication
Liquid carbon dioxide
Density enhancement
Cooling capacity
Machining
Energy effiency

ABSTRACT

Liquid carbon dioxide (LCO_2) based cryogenic cooling has shown promising results in terms of wear reduction, productivity increase and energy efficiency when machining high-temperature materials. For process-safe use with low pulsation, CO_2 must be fed in the liquid state to cool the process zone. LCO_2 is typically stored in riser bottles in which gaseous and liquid aggregate state coexist. A preliminary study has already shown that the liquefied state of the CO_2 can be stabilized by pre-cooling. In this paper, the influence of a heat exchanger as a pre-cooling system on the cooling capacity of the CO_2 is investigated and the required energy consumption is compared to unstabilized CO_2, pressure increased CO_2 and compressed air. It has been shown that pre-cooling leads to a more energy-efficient increase in the cooling capacity of the CO_2 compared to pressure increased CO_2.

1. Introduction

Among many other applications, CO_2 can be used as a coolant in machining processes. In this case, liquid CO_2 (LCO_2) expands in the process zone between the tool and the workpiece and cools due to the Joule-Thomson effect [1]. Although CO_2 can be rarely found in industrial applications, there are several reasons to prefer CO_2 compared to conventional coolants. While conventional cooling lubricants require costly maintenance and disposal as well as permanently operating energy-intensive pumps [2], CO_2 – stored in riser bottles – can be transported to the process zone with very little effort. Furthermore, the use of CO_2 produces technically clean and virtually contamination-free workpieces and chips due to the complete evaporation of the cooling medium. Thus, in most cases no post-treatment is required for further processing of both. Particularly for difficult-to-cut materials such as titanium- or nickel-based alloys, this alternative strategy offers longer tool life, a more stable process and cost benefits due to more productive cutting parameters [3,4]. Combined with the fact that usually the CO_2 used is a co-product of other industrial processes (e.g. ammonia synthesis) this makes CO_2 more energy efficient and sustainable than conventional metal working fluids in flood cooling [5,6].

For a stable process with sufficient cooling, it is important to ensure that the CO_2 is delivered to the process zone in its liquid phase and does not change to the gaseous phase before. One way of stabilizing the liquid state is CO_2 pre-cooling. Pre-cooling can be achieved by means of heat exchangers [7]. In order to correctly assess the positive effect of the heat exchanger, its energy consumption must be compared with the effect of the increased cooling capacity.

2. State of the art

2.1. Properties of carbon dioxide

Carbon dioxide is an acidic, non-flammable, odourless and colourless gas that is present as a trace gas in the atmosphere, making up 0.04 % by volume. Its molar mass of 44.00098 g/mol makes it heavier than air, which gives it a suffocating effect. For technical applications, CO_2 is transported in its liquid state in pressurized gas cylinders (e.g. riser bottles). However, under atmospheric conditions ($\vartheta = 20\ ^\circ C$, $p = 1.013$ bar) this phase does not exist [1]. For this reason, the pressure and/or temperature of the CO_2 must be adjusted for liquefaction (see Fig. 1). When the LCO_2 is expanded to atmospheric pressure, the phase change to the gaseous state takes place with a decrease in temperature. The reason for this is the inversion temperature of CO_2 of approximately $\vartheta = 209\ ^\circ C$. Below this temperature, the phase change takes place with cooling. This phenomenon is also known as the Joule-Thomson effect.

As can be seen in Fig. 1, by cooling the CO_2 at constant pressure, the state can be shifted from the binodal curve to the stable liquid range. This can also be used to liquefy the gaseous CO_2 and reduce pulsation effects.

* Corresponding author.
E-mail address: trixi.meier@fau.de (T. Meier).

https://doi.org/10.1016/j.cirpj.2024.09.007
Received 4 April 2024; Received in revised form 6 September 2024; Accepted 7 September 2024
Available online 24 September 2024

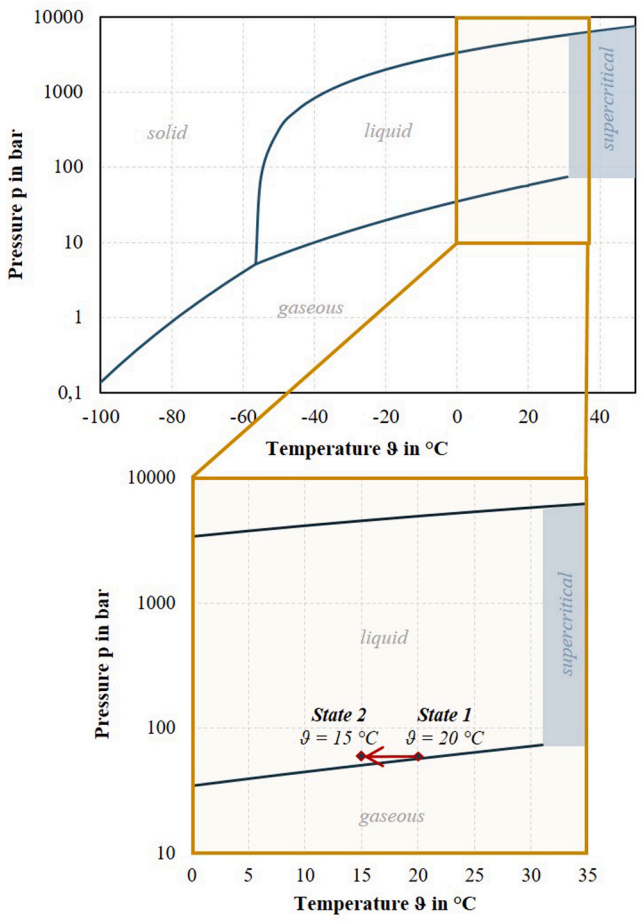

Fig. 1. p-ϑ diagram carbon dioxide.

2.2. Cryogenic cooling in machining

The most commonly used cryogenic media in machining are LCO_2 and liquid nitrogen (LN_2) [8–10]. Whereas LN_2 is the significantly colder medium ($\vartheta = -196$ °C compared to $\vartheta = -78.5$ °C for CO_2), its use is more complex. While it is possible to feed LCO_2, which is pressurized at $p = 57.29$ bar at ambient temperature ($\vartheta = 20$ °C), through uninsulated pipes, the entire pipe system must be insulated for LN_2 [1].

Gross has given an extensive overview on the topic of cryogenic cooling in machining, showing that the focus was mostly set on difficult-to-cut materials such as high alloy steels, titanium- or nickel-based alloys [11].

When using CO_2 as coolant, the reported results vary. *Jerold & Kumar* report lower cutting forces, reduced tool wear and improved chip breakability when turning AISI 316 stainless steel with CO_2 compared with wet and dry machining [12]. For milling of Ti-6Al-4 V *Tapoglou et al.* show higher tool wear and therefore a shorter tool life with CO_2 compared to flood cooling due to a lack of lubrication [13].

To mitigate this lack of lubrication the cryogenic minimum quantity lubrication (CMQL) has been developed and focused on in recent years. Here, a small quantity of oil is added to the cryogenic stream before it is applied to the machining process. The following references focus on CMQL using CO_2 as the cryogen.

Biermann et al. performed turning operations on the. Ti-alloys Ti-6Al-4 V and Ti-6Al-2Sn-4Zr-6Mo. They found that the use of CMQL improved the tool life and the chip breakability when compared to CO_2 or flood cooling. By comparing the results for both materials they concluded that the effectiveness of cryogenic cooling is highly dependent on the material properties [14]. *Villarrazo et al.* compared CMQL and MQL in a milling process of SISI 1045 carbon steel. While both showed similar cutting forces, CMQL allowed 18 % higher productivity and 30 % longer tool life [15]. Similar experiments were carried out by *Gross et al.* on Ti-6Al-4 V, comparing CMQL, MQL and flood cooling. At low cutting speed of $v_c = 70$ m/min they obtained minimum tool wear and cutting forces for MQL followed by CMQL and flood cooling. At higher cutting speed of $v_c = 130$ m/min CMQL provided the best results followed by MQL and flood cooling. These results led them to the conclusion that CMQL allows for a higher productivity than the alternatives studied [3]. Another group of researchers tested drilling processes on Ti-6Al-4 V and 42CrMo4 steel with CQML cooling and dry machining. For both materials a higher flow rate of CO_2 resulted in an increase in thrust force, due to the lower temperature. The use of sufficient oil for lubrication reduced the drilling torque significantly. For Ti-6Al-4 V the use of CO_2 alone already lead to a reduction in torque compared to dry machining, due to improved chip evacuation. This improved evacuation was made possible by better chip breakability and therefore chip morphology was reported under cryogenic machining. [16]; [17].

As explained in 2.1, cooling the CO_2 can be used to stabilize its liquid phase. Another way to obtain a CO_2 with stable conditions is to increase its pressure and temperature beyond the critical point ($\vartheta = 31.0$ °C, $p = 73.8$ bar) to where it becomes supercritical ($scCO_2$), which is also shown in Fig. 1 [18]. Similar to LCO_2 the addition of MQL in combination with $scCO_2$ is used to facilitate cooling and lubrication of the cutting process. A study by *Wika et al.* compares $scCO_2$ +MQL and flood cooling in terms of tool life and material removal volume when milling AISI 304 L stainless steel. In both categories $scCO_2$ +MQL significantly outperformed flood cooling [19]. In comparable studies on milling Ti-6Al-4 V *Khosravi et al.* and *Tapoglou et al.* also reported increased tool life with $scCO_2$ +MQL compared to flood cooling or CO_2 alone. Additionally *Khosravi et al.* reported improved surface integrity and lower cutting forces [20]; [21]. In another study *Stephenson et al.* likewise compared $scCO_2$ +MQL with water-based flood cooling when rough turning Inconel 750 [22]. They also reported lower tool wear and a higher material removal rate for the combination of $scCO_2$ and MQL.

To ensure the supercritical state of the CO_2, appropriate system technology is required. Pressure and temperature must be controlled throughout the entire supply line. It is therefore important to prepare the machine tool sufficiently for the use of $scCO_2$. The homogeneous miscibility of CO_2 and oil is a basic assumption for the use of $scCO_2$.

Nevertheless *Meier et al.* investigated the static and dynamic solubility of various bio-based and synthetic oils with LCO_2. The results showed that some oils have a complete solubility in LCO_2, some oils showed a partial solubility and other oils did not mix with LCO_2 at all and were present in two completely separate phases. However, all three different solubility classifications of the oils showed very good results in oil application as well as good cutting results with geometrically defined cutting edges. No clogging occurred (proof by continuous oil application), which can be explained by the high pressure and speed of the LCO_2 in the supply line and even if there are two separate phases of oil and LCO_2, both media are present in the liquid state. The pressure of the oil supply line is always higher than the LCO_2 so that it can be injected into the LCO_2 at the mixing valve. The oil application tests and machining tests were carried out both with an external coolant supply with a round nozzle with $d = 0.2$ mm and $d = 0.3$ mm and with an internal coolant supply through the milling or drilling tool with different coolant channel diameters in the range of $d = 0.25/0.5/0.75$ mm. Furthermore, bio-oils can be used for CMQL, which are otherwise hardly used or not used at all in machining due to their tendency to oxidize and polymerize. This can therefore make an important contribution to the sustainability of machining processes. [23]; [24].

2.3. Existing CMQL-Systems for CO_2

This chapter presents CMQL-systems that are already available on

the market and can therefore be purchased by companies. In addition, there are other systems that are currently only the subject of research and are being developed at various research institutes worldwide, as well as other systems in the further development stage of systems that are already commercially available and systems with patent status. In their publication, *Iruj et al.* provide a detailed overview of the present status of CMQL-systems and their performance and machine integration [25].

The following Table 1 provides an overview of CMQL-systems already available on the market and classifies them according to the aggregate state of the CO_2.

The company Fusion Coolant Systems uses $scCO_2$ in its *PureCut+* system. In this state, it exhibits the flow and expansion behavior of gases, while at the same time being able to completely dissolve liquids. This property enables improved dissolution and mixing of the oil with the $scCO_2$, assuming the oils used are soluble in $scCO_2$. To bring the LCO_2 to the supercritical state, the LCO_2 is first increased to the critical pressure using a pressure booster (e.g. pump). The CO_2 is then heated to the critical temperature and transferred to the supercritical state. The two media (oil and $scCO_2$) are mixed in a chamber. The additional modification of the CO_2 increases the complexity of the system and requires that the oils used can be dissolved by the $scCO_2$ in order to ensure transport to the cutting zone. [26].

Cool Clean Technologies' commercial system *ChilAire* is based on the introduction of liquid and gaseous CO_2 in separate pipes, which are then mixed together. The result is a fluid with a temperature range of $\vartheta = -7\ °C$ to $\vartheta = 21\ °C$ and a pressure range of $p = 5$ bar to $p = 69$ bar. The addition of a processing oil is optional, whereby the commercial focus of the system is on pure CO_2 processing [27].

The company HRE Automation offers a CMQL-system called *BeCold*. The *BeCold* system consists of a self-developed CO_2 cooling unit and an existing MQL-system from SKF called "LubriLean". The LubriLean system generates a compressed air flow containing finely dispersed oil droplets, which are directed to the cutting zone. This system can be used for both internal and external MQL. With internal lubrication, the LubriLean system generates an oil-air mixture in the oil reservoir and directs it to the cutting zone either through the rotating spindle or through the tool revolver. With external MQL, the lubricant is atomized by compressed air in a spray nozzle, forming micro-droplets, which are directed to the cutting zone with the help of the so-called spray air. The CO_2 is added to the oil-air mixture shortly before it exits the nozzle and has a liquid aggregate state when combined [28].

The *AerosolMaster 4000 Cryolub* system, developed by Knoll Maschinenbau (formerly marketed Rother-Technologie), uses a pressurized container to generate a fine oil-air mixture for the MQL. This mixture is fed through the main line to the tool holder. The LCO_2 is transported separately in a second capillary line. With internal cooling lubrication, the oil-air mixture and the LCO_2 are mixed in the tool holder. For external cooling, Knoll integrates a parallel expansion nozzle at the end of the main line, which transports the oil-air mixture in the outer channel and has a second channel for the LCO_2 integrated inside. No prior mixing is provided, which means that the system makes machine tool integration more difficult due to the two-channel supply [29].

As the presentation of the state of the art and the list of CMQL systems shows, there have been many studies in recent years on the use of CO_2 for cryogenic cooling in machining with focus on process parameters, wear and CO_2-oil miscibility. The cooling performance compared to other coolant strategies has only been investigated to a limited extent with low comparability due to the different test setups and the different CMQL-systems. In a study, *Pušavec et al.* investigated the cooling capability of LCO_2 in comparison to LN_2 and emulsion. Therein, the cooling capacity of the three strategies is directly related to the mass flow of the coolant. They find that while the cooling effect of the cryogens is caused by their phase transition, the cooling capacity of emulsion is positively correlated to the temperature difference. [30].

Most manufacturers recommend the use of riser bottles or packs of riser bottles. However, a high LCO_2 quality is assumed as a precondition for most investigations. The research gap described in this paper therefore deals with the LCO_2 supply and the associated problems of the changing and unstable initial states of the LCO_2 when working with riser bottles or packs of riser bottles. The investigation of pre-cooling of the LCO_2 to increase the density is compared with pressurized CO_2 (alternative for stabilization) in terms of the cooling capacity and the energy consumption required to stabilize the LCO_2.

Table 1
Commercial CMQL-systems for CO_2.

CMQL- system	Company	Aggregate state CO_2
PureCut+	Fusion Coolant Systems	supercritical
ChilAire	Cool Clean Technologies	gaseous liquid
BeCold	HRE Automation	liquid
AerosolMaster 4000 Cryolub	Knoll Maschinenbau	liquid

3. Experimental setup

This chapter describes both the initial CO_2 supply situation and the experimental setup of this study. The cryogenic mixing system used, the cooling capacity measurement setup and the design of experiments are explained in more detail.

3.1. Carbon dioxide supply

One problem observed at the REP institute is the lack of knowledge about the filling level of the liquid portion of the CO_2 in riser bottles. With the help of the thermodynamic law of the lever and the relationship from the ϑ-s diagram, a functional relationship can be derived between the withdrawal of LCO_2 and the two states of a new riser bottle and one bottle that is at a critical filling level. Since the withdrawal tube of the riser bottle extends to approx. 5 cm from the bottom of the bottle, the withdrawal of liquid phase can only be guaranteed for a filling level of LCO_2 up to the tip of the withdrawal tube. Progressive removal of liquid phase from the riser bottle creates more space for the expansion of liquid phase into gaseous phase, which additionally reduces the liquid phase of the CO_2 within the riser bottle (see Fig. 2).

As an example, the volumes for liquid and gaseous states are shown proportionally, as well as how these change during the course of the extraction. Since the absolute volume of the riser bottle is known to be 50 liters and the mass of CO_2 contained at delivery is 37.5 kg, the specific volume of the delivery state can be calculated by dividing the two variables. Subsequently, the thermodynamic law of the lever provides the knowledge that at the beginning approx. 1 % of the delivered CO_2 is in a gaseous state, as it is not technically possible to fill the cylinder with 100 % LCO_2. The volume of the liquid phase can be calculated, up to which filling level the tip of the withdrawal tube is completely surrounded by LCO_2. On the basis of the assumptions made, LCO_2 can be withdrawn safely until a gas content of 96.2 % is reached in the riser

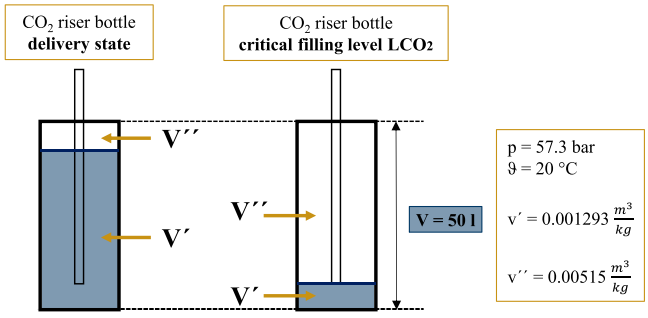

Fig. 2. Delivery state vs. critical filling level of a CO_2 riser bottle.

bottle. This translates to a mass of 26.69 kg which can be withdrawn safely in liquid state. The remaining CO_2 is already in the gaseous state at this point or in a liquid state but below the tip of the withdrawal tube. This information can now be related to the mass flow of the withdrawal, which makes it possible to determine a time until LCO_2 can be taken safely from the riser bottle.

The filling level of a riser bottle can therefore also be determined by weighing. Here, the residual weight of the gas phase and the LCO_2 below the riser tube calculated above must be included in the calculation or subtracted from the usable LCO_2. Weighing a single riser bottle is possible with little effort and could also be realised as a continuous measurement. However, weighing a pack of riser bottles with 12 individual bottles connected in a steel cage weighing over 1.2 tons is more complex and measurement accuracy is reduced. In addition, weighing the entire pack does not allow any conclusions to be drawn about the individual riser bottle. This is problematic if, for example, individual bottles are defect (e.g. shorter broken riser tubes) or if, during continuous operation with the pack, individual bottles are emptied more than others (e.g. due to the distance to the extraction point (valve of the pack). These problems were frequently observed in tests carried out by the REP institute. According to the measured weight, the pack should still be more than half full with usable LCO_2, but a significantly lower density is measured with a Coriolis sensor directly at the valve of the pack, which confirms a high gas phase content. This problem has also been confirmed with various CO_2 suppliers and various types (in terms of the pipework of the individual bottles as a pack) of riser bottle packs. A few packs show a similar problem already a short time after the pack has been completely filled, with a significantly lower CO_2 density.

It is important that the pressure is not considered as a parameter for the filling level of the CO_2 cylinders, as it remains constant due to the conversion of liquid CO_2 into gaseous CO_2 in the bottle.

It is also possible to define a critical density at which it becomes clear to the user that not only LCO_2 is being withdrawn from the riser bottle. Regarding a density of approx. $\rho = 200$ kg/m^3 there is only pure gaseous phase in the supply line and no LCO_2 which can expand at the outlet. The density of the extracted substance can be measured with a Coriolis sensor, which should be connected upstream of a CMQL system. In addition, after removal from the riser tube cylinder, it must be ensured that the internal diameter of the supply line remains constant or becomes smaller towards the outlet or nozzle. This prevents the formation of a two-phase flow due to pressure changes caused by diameter expansion (conversion of LCO_2 to gaseous CO_2). This conversion leads to a lower average density of the two-phase flow.

The CMQL mixing unit of the REP institute is equipped with a Coriolis sensor to monitor and record the CO_2 density. However, simply monitoring the density is not sufficient for a series application. Because if a low density is measured, it is already too late and the machining process is no longer sufficiently cooled. The density of the CO_2 must therefore be increased before it reaches the cutting zone. One way of doing this is to pre-cool the CO_2, which is described in more detail in the following section on the structure of the cryogenic mixing unit used for this investigation.

3.2. Cryogenic mixing unit

Preliminary studies at the REP institute have shown that no supercritical or gaseous state is required to use CO_2 as a carrier medium for a CMQL technology. In the 1-channel CMQL system developed at the REP, LCO_2 is extracted from riser bottles.

A high performance liquid chromatography pump (HPLC) delivers an oil, which is injected into the CO_2 stream and transported to the process zone as an emulsion or two-substance mixture. The unit can be implemented with external coolant supply as well as with internal coolant supply through the tool and it can provide either pure cryogenic cooling, CMQL or standard MQL. [11; 31].

In the mixing unit itself, the oil volume flow is regulated via the control of the HPLC dosing pump. The CO_2 mass flow, temperature and density are measured via a Coriolis sensor and shown on a display. Digital control of the system is possible with the aid of an external control unit. The LCO_2 flow is regulated by the nozzle diameter. In this test setup, a round nozzle with an outlet diameter of $d = 0.2$ mm is used. This generates a LCO_2 flow of $\dot{m} = 5$ kg/h (measured by the Coriolis sensor installed in the mixing system). The control unit enables the oil dosing pump and the CO_2 supply to be switched on and off and can also be connected to the CNC machine control system to be activated via the machining program code. The oil flow rate can be adjusted from 0.06 ml/h up to 600 ml/h via the HPLC pump. The recorded values of the oil and CO_2 supply are displayed on a dashboard with automatic data storage.

The temperature and pressure conditions during the supply of the two media shown in Fig. 3 illustrate the changes in the CO_2 aggregate state within the system. It can be seen that the CO_2 is kept at $\vartheta = 20$ °C with a pressure of $p = 57.3$ bar during extraction which is measured using a Coriolis and a pressure sensor and is in agreement with the theoretical values from the p-ϑ diagram.

The oil pump must generate a counter pressure in order to be able to inject the oil into the liquid CO_2 stream. The CO_2 remains in this state until it enters the nozzle (1). Inside the nozzle (2), the pressure level is equalized by the atmospheric pressure upstream of the nozzle. The pressure drops to $p = 5.18$ bar, with a drop in temperature to $\vartheta = -56.6$ °C. At the triple point reached in this way, the CO_2 is present in the three aggregate states of gaseous, liquid and solid. Atmospheric pressure of $p = 1.013$ bar prevails directly at the nozzle outlet (3). At this point, the CO_2 reaches its minimum temperature of $\vartheta = -78.5$ °C.

For a process-safe application of the system with low pulsation, the CO_2 must be in a liquid state at the unit inlet. Changes in the ambient conditions, e.g. lower temperature, low CO_2 level or defects in riser pipes, can lead to an increasing gas phase proportion and a lower CO_2 density. As already mentioned, a preliminary study on increasing the density by pre-cooling the CO_2 supply line was carried out at the institute.

The aim of CO_2 pre-cooling is to maximize the liquid fraction of CO_2 that arrives at the mixing valve of the 1-channel CMQL unit. As the cooling effect of the CO_2 is primarily generated by sublimation, this can be optimized by subsequent liquefaction of the CO_2 in the feed. In the preliminary study, cooling is carried out using a cooling circuit in which a water tank ($V = 8$ l) is cooled with a heat exchanger to a constant temperature of $\vartheta = 4$ °C = 4 °C and the CO_2 is fed through a pipe with a length of $l = 3$ m. With this cooling process, the CO_2 (mass flow rate of $\dot{m} = 5$ kg/h) could be cooled from the initial temperature $\vartheta = 21$ °C to $\vartheta = 14.84$ °C and the density increased from $\rho = 550$ kg/m^3 to over $\rho = 800$ kg/m^3 , see Fig. 4.

The heat exchanger is also able to cool higher mass flows of LCO_2. This test setup (8 l water tank and cooling supply line length of $l = 3$ m) has already been tested positively for LCO_2 mass flows of up to $\dot{m} = 12$ kg/h. With higher mass flows, the flow velocity and the mass flow must always be considered. Depending on this, the water temperature must be reduced or the cooling supply line length simply extended.

The thermodynamic relationships when cooling the CO_2 after it leaves the riser bundle are explained using the ϑ-s diagram in Fig. 5.

Initial state 1 ($\vartheta = 20$ °C, $p = 57.3$ bar, $\rho = 500$ kg/m^3) characterizes the CO_2 as it exits the bundle of riser bottles and describes a state within the wet vapor region. If a cooling effect is applied to the CO_2 at constant pressure, the density increases as the temperature falls (state 2). This moves the CO_2 state over the boiling line, so that a stable liquid state is achieved. This heat exchanger is also used for the following cooling capacity measurement. In contrast to the preliminary study, the water temperature of the heat exchanger is now adjusted adaptively in this investigation.

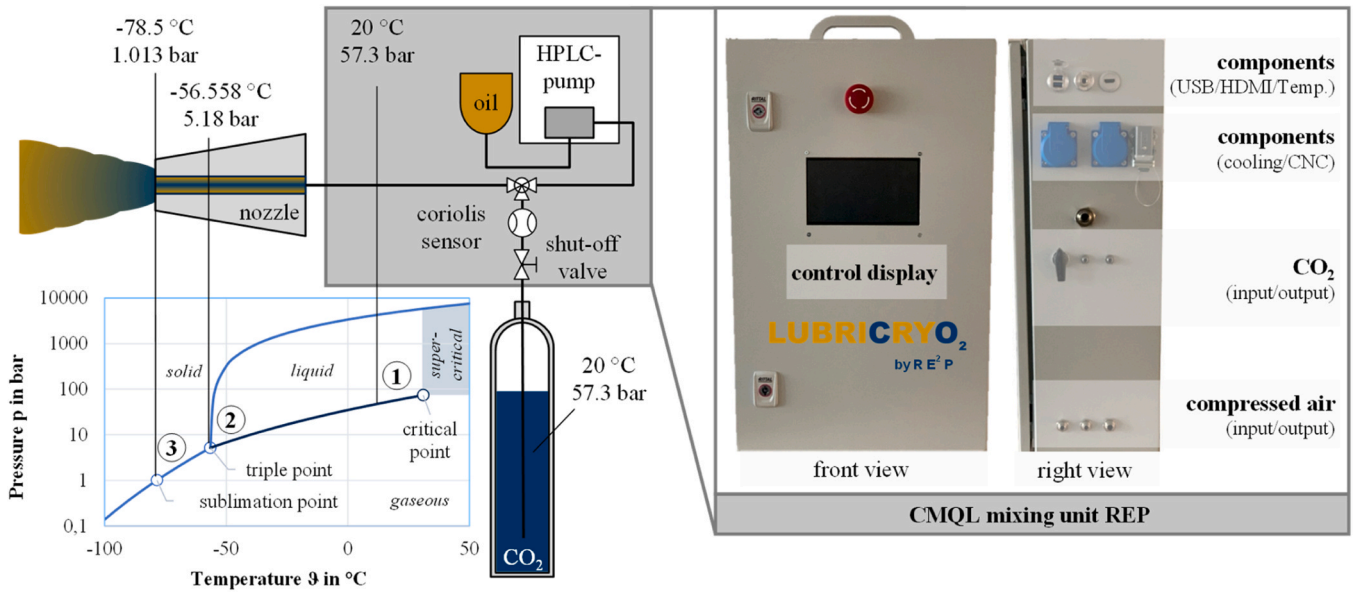

Fig. 3. CMQL unit LUBRICRYO$_2$ of the REP institute.

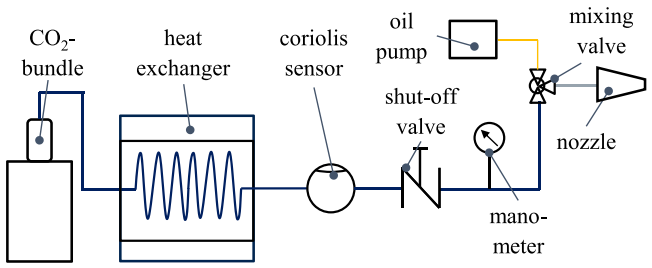

Fig. 4. CMQL unit LUBRICRYO2 with CO_2 pre-cooling.

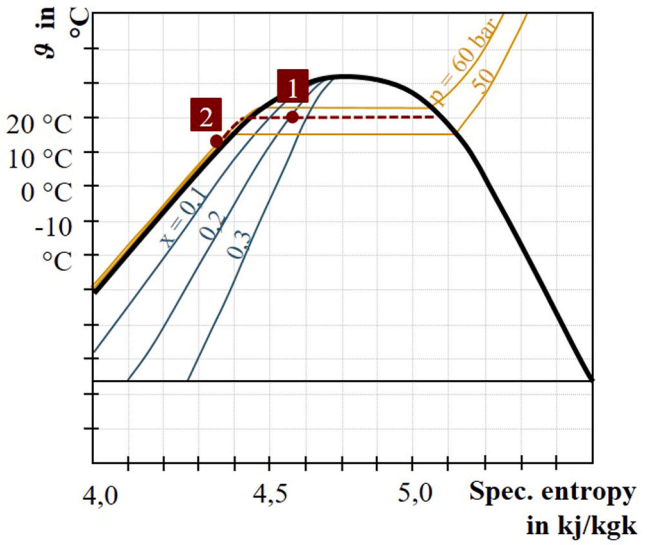

Fig. 5. ϑ-s diagram CO_2.

3.3. Cooling capacity measurement

The cooling capacity measurement represents a first approach to quantify the cooling effect of expanding LCO_2. This enables a categorization of system parameters that can be tailored to the desired cooling conditions for a distinct machining process. In an attempt to reduce disruptive factors, a test setup outside of the process zone is designed.

The elemental parts to this setup are a heating resistor and a Voltcraft current clamp of the type RS CP-10. The heating resistor limits its power consumption according to its temperature. In turn, the electric current rises when the heating resistor is cooled down externally by CO_2. After a ramp up, the consumed power correlates with the cooling capacity of the CO_2. The heating panel requires a constant voltage of U = 24 V DC, which simplifies the calculation of the power consumption to:

$$P = U \cdot I$$

The heating resistor has the dimensions of 75 × 25 mm. Depending on its temperature, the resistance lies between R = 4.3 Ω and R = 51.1 Ω. Without any cooling, the heating resistor reaches a maximum temperature of T_{max} = 110 °C. This is considered the point of stable power consumption of P = 15.2 W which marks the CO_2 valve opening and thus the start of the experiment. The cooling capacity is calculated by:

$$P_{Cooling} = P_{Heating} - P_{Stable}$$

The current clamp is connected to a voltage measurement port of the NI measurement card PXIe-6341 which is suitable for measurement applications. Three cable windings are inserted into the clamp to average the current. The measurement and storage of the data is performed by applying a LabVIEW program. As mentioned above, the characteristics of the CO_2 stream are recorded through the integration of a Coriolis sensor of the type Cori-Flow M14 by Bronkhorst. It is positioned inside the aforementioned cryogenic mixing unit and delivers information such as the temperature, the density as well as the flow rate of the CO_2. The connection of this sensor via RS232 interfaces allows an inclusion of the measurement into the same LabVIEW program and thus a synchronized data set in the same data file. An additional thermocouple is located at the heating panel to directly observe the temperature while cooling in case there is a hardware dependent power maximum. Furthermore, a K-type thermocouple is integrated between the cables and the metal housing of the heating panel. A similar test set up is developed by *Pušavec et al.* [30]. Therein, the heat is generated by a heating coil that enables the realization of multiple stable temperature levels instead of a heating resistor that leads to a single equilibrium between heating power and cooling capacity. While both set ups correlate the heat transfer rate of the heater to the cooling capacity, the

heating resistor in the present study has a larger surface to ensure that the CO_2 stream completely reaches the heated area.

As depicted in Fig. 6 the CO_2 nozzle as well as the heating panel are fixed by magnetic holders. For stability purposes the original clamps are replaced by screws.

3.4. Design of experiments

The experiments for the characterization of the impact of the water temperature on the cooling capacity are carried out with a nozzle diameter of d = 0.2 mm. In addition, the influence of the nozzle distance to the heating panel is studied for the nozzle heights h = 2 cm to h = 10 cm. The optimum distance in which the CO_2 stream reaches the panel but can also expand before impact is h = 4 cm. Therefore, this distance is applied for the investigation of the pre-cooling water temperatures that are responsible to cool the CO_2. Experiments start at a temperature of $\vartheta = 16$ °C and progress in 2 °C steps down to $\vartheta = 2$ °C. At the beginning of each iteration of the experiment, the panel is entirely heated up until a point of stable power consumption is reached. This ensures identical starting conditions for each measurement and gives an indication for the maximum power achievable by the heat resistor. After opening the CO_2 valve and a following rise in power consumption, a relatively stable phase of cooling capacity is reached. These investigations are complemented by the pressurization of the LCO_2 without any pre-cooling on the pressure levels of p = 100 bar, p = 150 bar and p = 200 bar with an inert gas dosing device DSD 500 by Maximator GmbH and Linde AG. An overview of these boundary conditions is given in Table 2.

4. Results

4.1. Influence of the nozzle distance on the cooling capacity

First, the influence of the nozzle distance is considered in the described experimental setup in Fig. 7 for CO_2 without pre-cooling. Therein, the cooling capacity shows a clear dependence on the nozzle distance. However, the cooling capacities for distances h = 0.5 cm and h = 2 cm do not differ substantially. As these are the realistic distances to the tool when integrating the nozzle into the process zone, this minimal variance is considered beneficial, since it simplifies the installation.

Afterwards, the cooling capacity reaches a stable state for nozzle distances h = 4 cm to h = 8 cm. In this range, a lower cooling capacity is observed that is still considered applicable. For distances larger than h = 10 cm, the CO_2 does not reach the heating plate continuously. There is still some cooling effect due the now fully evaporated CO_2 and cooled air in the surrounding, however, these distances are not recommended for a practical application.

As the following study focuses on the behavior of the CO_2 stream under various conditions, a medium distance of h = 4 cm is selected for the following experiments. This ensures, that the CO_2 stream fully reaches the heating plate. Additionally, differences in the cooling capacity become easier to measure than with lower nozzle distances.

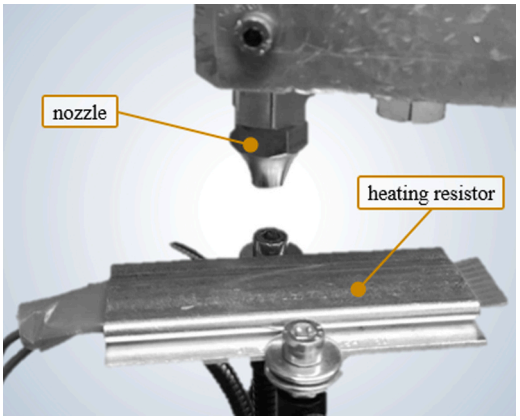

Fig. 6. Experimental setup cooling capacity measurement.

Table 2
Overview of the boundary conditions for the CO_2 experiments.

Dimensions	Values
Nozzle diameter d (mm)	0.2
Nozzle distance h (cm)	2, **4** (default), 6, 8, 10, 12, 14
Water temperature ϑ (°C)	16, 14, 12, 10, 8, 6, 4, 2
Heating panel dimensions (mm)	75 × 25
Heating panel current (V)	24 DC
Heating panel resistance (Ω)	4.3 – 51.1
Pressure (bar)	**57.3** (default), 100, 150, 200

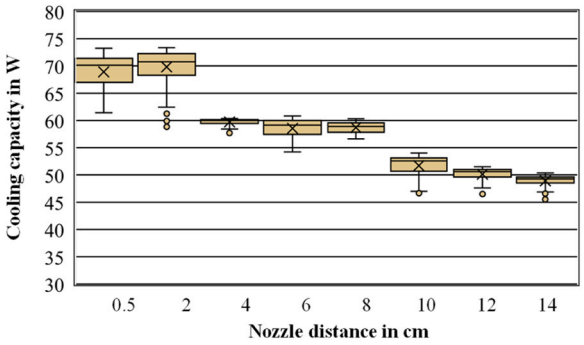

Fig. 7. Dependency of the cooling capacity on the nozzle distance.

4.2. Effects of CO_2 pre-cooling on the cooling capacity

As shown in Fig. 8, the density of the CO_2 is drastically improved by any amount of pre-cooling. Afterwards, it is steadily increasing with falling pre-cooling temperatures. Furthermore, the variance of the density is a positive remark for every pre-cooling temperature, as it decreased from $\rho = 50$ kg/m^3 in processes without any pre-cooling to $\rho = 5$ kg/m^3 for every pre-cooling temperature. The observed increase in density does not allow any direct conclusions regarding the cooling capacity. In fact, comparing the diagrams in Fig. 8 and Fig. 9 suggests that a density above around $\rho = 800$ kg/m^3 is not beneficial for a heightened cooling capacity. While minor improvements above this point are technically possible through intensive pre-cooling, the effort does not appear reasonable.

The benefit of higher densities lies within the increase in flow rate without having to integrate mechanical valves that lead to an expansion of the CO_2 within the pipe system. The pre-cooling of the CO_2 can thus be applied to raise the flow rates dynamically. The relation of flow rate

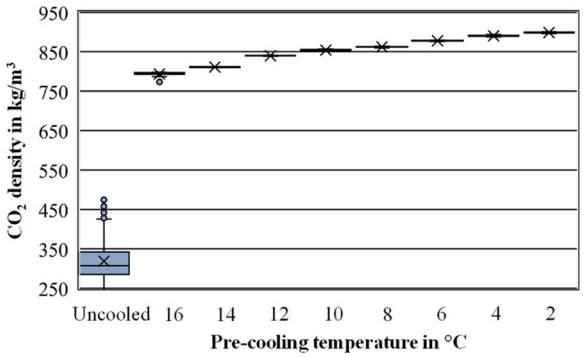

Fig. 8. Impact of the pre-cooling temperature on the CO_2 density.

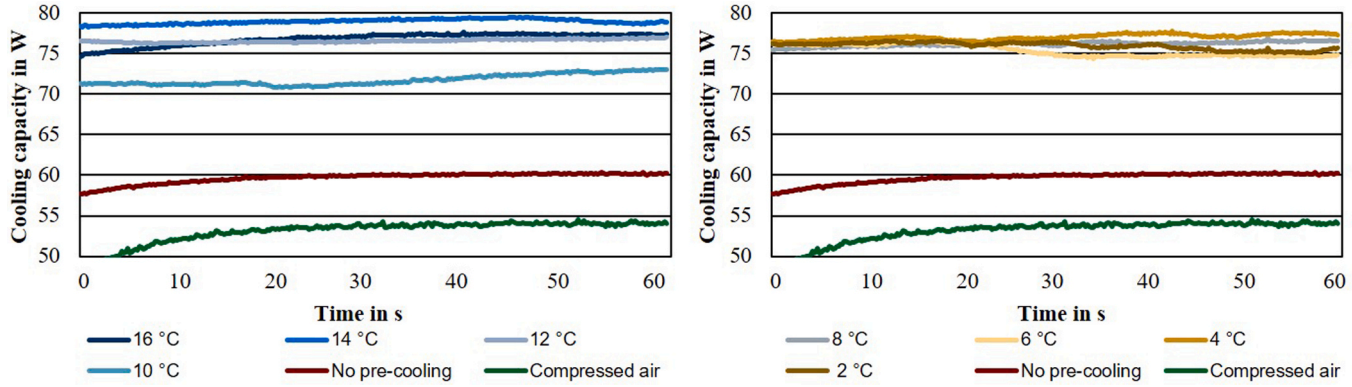

Fig. 9. Influence of the pre-cooling temperature on the cooling capacity.

and pre-cooling temperatures is shown in Fig. 10.

Similarly to the density, the flow rate varies greatly in an uncooled state, signifying the need to stabilize the LCO_2-stream. Its median value of $\dot{m} = 1.8$ kg/h is improved by 322 % up to $\dot{m} = 5.8$ kg/h for pre-cooling temperatures of $\vartheta = 2$ °C. However, based on Fig. 9 it can be reasoned that a variation of the flow rate of $\dot{m} = 1$ kg/h does not drastically influence the cooling capacity. If the machining processes were to require even higher cooling capacities / flow rates, a higher nozzle diameter or pressurization of the LCO_2 would have to be applied.

Fig. 9 shows the cooling capacity at different pre-cooling temperatures in comparison to the reference without pre-cooling. The cooling capacity is depicted after a ramp up time of approximately t = 1 min once it reaches quasi stable conditions. For a CO_2 supply without any pre-cooling the cooling capacity lies at a maximum of P = 60 W. In comparison, an alternative cooling strategy without lubrication through pressurized air achieves a cooling capacity of P = 54 W. Therein, a larger nozzle diameter of d = 0.5 mm is applied for a sufficient air flow. This leads to a volume flow rate of V = 1.8 m^3/h at a pressure level of p = 9 bar. This combination results in an average of P = 54 W, which equals a loss of 10 % cooling capacity compared to uncooled LCO_2. Its efficiency is drastically decreased to 70 % when contrasted with the average cooling capacity of pre-cooled configurations.

The cooling capacity of pre-cooled CO_2 exceeds the cooling capacity of non pre-cooled CO_2 in every experiment. The lowest cooling capacity of P = 70 W can be observed for a water temperature of $\vartheta = 10$ °C. A maximum cooling capacity is measured at a pre-cooling water temperature of $\vartheta = 14$ °C at P = 80 W. It appears that a further lowering of the pre-cooling temperature does not influence the cooling capacity significantly.

For a further analysis of this behavior, the temperature of the heating panel is visualized in Fig. 11. While the median temperatures differ from

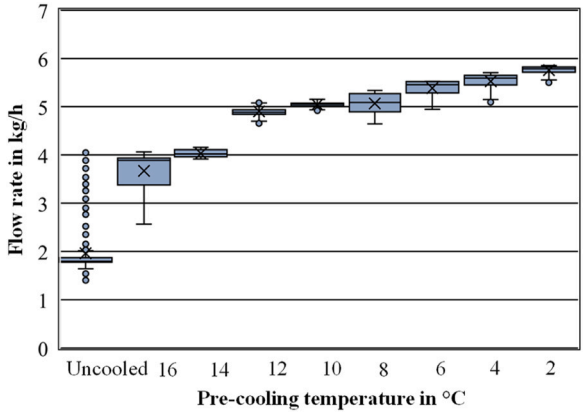

Fig. 10. Correlation between pre-cooling temperature and CO_2 flow rate.

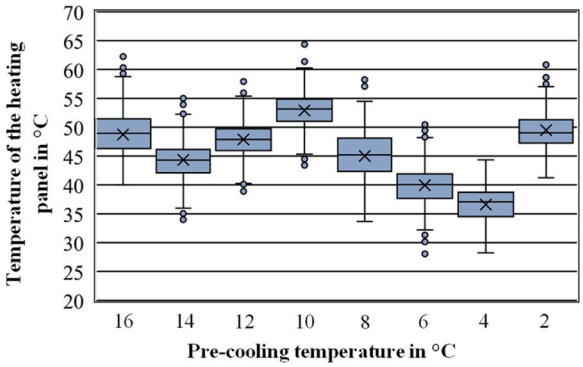

Fig. 11. Temperature of the heating panel during cooling with pre-cooled CO_2.

$\vartheta = 53.2$ °C for a pre-cooling temperature of $\vartheta = 10$ °C to $\vartheta = 36.5$ °C for a pre-cooling temperatre of $\vartheta = 4$ °C, there is no clear correlation between the heating panel temperature and the pre-cooling temperature. The highest temperature at $\vartheta = 10$ °C fits the low cooling capability curve of this pre-cooling temperature in Fig. 9. Furthermore, similar temperatures of the heating panel for $\vartheta = 12$ °C and $\vartheta = 8$ °C also exhibit a similar cooling capacity. However, the lowest panel temperature for $\vartheta = 4$ °C does not lead to the highest cooling capcity. This indicates a suboptimal measurement resolution that can only be used for a first qualitative estimation and will be improved in future research.

Another advantage of the pre-cooling of LCO_2 is the reduction of the ramp up time from the opening of the CO_2 valve until a stable level of cooling capacity is reached. It is possible to verify this theory by utilizing the same experimental setup. For this purpose, the measurement files are extracted in the range from P = 20 W to P = 80 W. The former represents the standardized valve opening point. The limit of P = 80 W is chosen arbitrarily as a value that is reached for every pre-cooling temperature. The results are depicted in Fig. 12. It is apparent that the slowest increase occurs at a pre-cooling temperature of $\vartheta = 16$ °C which is also caused by the initial ramp up. In contrast, the fastest increase is performed at $\vartheta = 2$ °C. This indicates a verification of the aforementioned theory. However, the remaining measurements do not follow the same trend, with $\vartheta = 10$ °C having the second slowest rise. This might be explainable by the comparatively low maximum at this temperature and a therefore earlier flattening of the curve. The evidence in total does neither support nor deny the thesis. It remains to be seen how this property behaves in future studies.

4.3. Increasing the cooling capacity by pressurizing the LCO_2

Pressurizing the LCO_2 is a suitable alternative to pre-cooling when aiming to stabilize the liquid phase. The inert gas dosing device DSD 500

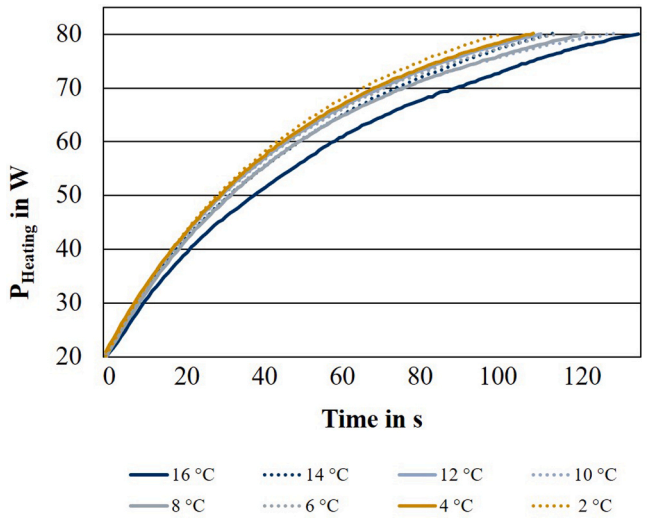

Fig. 12. Increase in cooling capacity.

by Maximator GmbH and Linde AG enables a re-compaction of the CO_2 stream to p = 500 bar. By doing so, the density reaches very homogeneous levels just below ρ = 900 kg/m^3. Fig. 13 shows the cooling capacity for the pressure levels p = 100 bar, p = 150 bar and p = 200 bar in comparison to the initial state. The nozzle distance is kept constant at h = 4 cm as well as the nozzle diameter at d = 0.2 mm.

The pressurization shows a decisive influence on the cooling capacity with the lowest median for p = 100 bar at P = 114 W. An additional increase in pressure leads to higher cooling capacities of up to P = 122 W for p = 200 bar. However, the gap is not as large. This is also reflected in the temperature of the heating panel in Fig. 14.

In comparison to the pre-cooling of the LCO_2, lower heating panel temperatures are reached with the smallest median of ϑ = 15.3 °C at p = 150 bar. According to this, an equipment dependent minimum temperature is not reached before in Fig. 11. However, this limitation of the measurement system might now be met, as there is no visible temperature difference between p = 150 bar and p = 200 bar. The higher pressures are also connected to a drastic rise in flow rate as is shown in Fig. 15. The variation in flow rate for the pressurized curves is caused by the speed of the piston in the re-compaction process. The median flow rate rises to ṁ = 11.7 kg/h for p = 100 bar, while even reaching ṁ = 18.8 kg/h for p = 200 bar. Thus, the re-compacting of the LCO_2 becomes an economic aspect due to the higher flow rates that needs to be considered for a practical application.

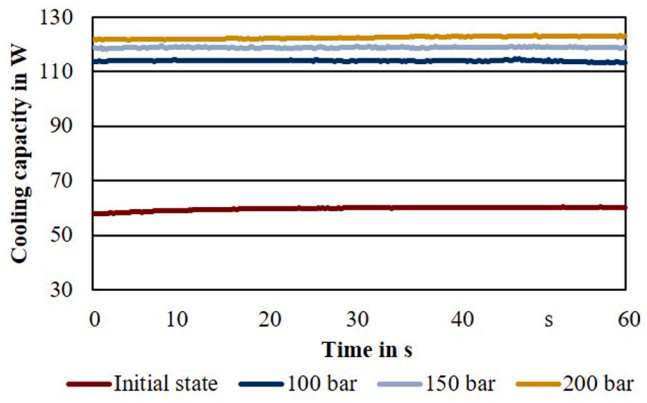

Fig. 13. Cooling capacity for pressurized LCO_2.

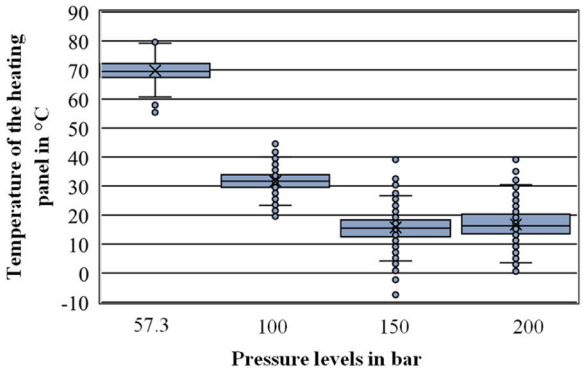

Fig. 14. Temperature of the heating panel under pressurized CO_2 cooling.

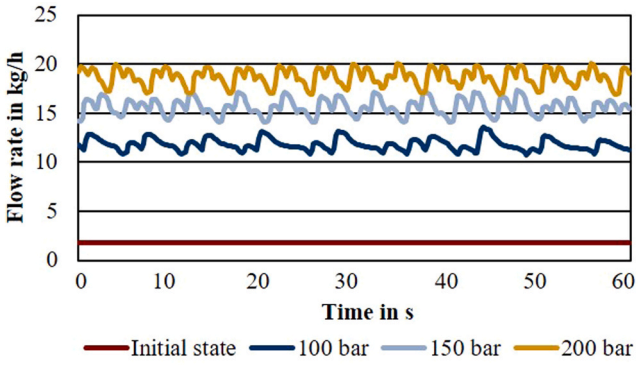

Fig. 15. CO_2 flow rate for various pressure levels.

4.4. Consideration of energy consumption

The previously described measures of pre-cooling and pressurization alter the properties of the LCO_2 in a way that leads to an increase in flow rate. Hence, the cooling capacity is improved by utilizing higher amounts of LCO_2. A general overview of the energy efficiency is given by calculating the specific cooling capacity P'_p for each parameter variation in Table 3.

The specific cooling capacity P'_p is calculated as follows:

$$P'_p = \frac{P}{\dot{m}}$$

The highest specific cooling capacity is achieved by the initial state without pre-cooling or additional pressurization because of its low flow rate. The comparatively low cooling capacity in this state and the pulsation caused by high flowrate and density variations is improved through the described measures. However, the cooling capacity does not increase at the same extend as the flow rate which leads to a lower specific cooling capacity. For pre-cooling, the specific cooling capacity remains moderately high with the best values for pre-cooling

Table 3
Specific cooling capacity P'_p for each factor variation.

ϑ_{Water} (°C)	Pressure (bar)	ṁ (kg/h)	P (W)	Specific cooling capacity P'_p (Wh/kg)
/	initial state	1.8	60.0	33.33
16		3.9	76.8	19.69
14		4.1	79.0	19.27
12		5.0	76.6	15.32
10		5.1	71.7	14.06
/	**100**	11.7	114.0	9.74
/	**150**	15.6	118.9	7.62
/	**200**	18.8	122.5	6.52

temperatures of $\vartheta_{Water} = 16$ °C. By further increasing the pressure of the LCO_2, the flow rates rise strongly which results in a reduction in the specific cooling capacity. Thus, the pressurization appears to be connected to a lower CO_2 efficiency.

To further evaluate this aspect, the energy consumption of the cryogenic mixing unit and the inert gas dosing device DSD 500 by Maximator GmbH and Linde AG are measured additionally. For this purpose a power supply measurement device of the type Qualistar+ C. A. 8336 by Chauvin Arnoux is connected to the system. Since the cooling process of the mixing unit is regulated by the water temperature, the energy consumption $E_{measured}$ is measured over a time frame of t = 1 h to even out the numerous reheating and cooling down cycles. This time frame is also used for the calculation of the additional energy consumption E_{add} and the total energy consumption E_{total} in Table 4. The measurement is performed without CO_2 to avoid futile emission. For a realistic estimation, the heat flux of the CO_2 is then added to the measured energy consumption.

$$E_{total} = E_{measured} + E_{add}$$

The additional energy consumption through the heat flux of the CO_2 is calculated by:

$$E_{add} = \Delta T \bullet \dot{m} \bullet c_p' \bullet t$$

According to [1] the specific heat capacity of CO_2 is c_p' = 4.264 kJ/(kg K).

This experiment is limited to the pre-cooling temperatures $\vartheta = 16$ °C to $\vartheta = 10$ °C because even lower temperatures do not lead to a higher cooling capacity as shown in section 4.1 and is therefore not recommended. The values for the temperature ϑ_{CO2} as well as the flow rate $\dot{m}$ of the CO_2 have been recorded by the Coriolis sensor in previous experiments. The results are shown in Table 4.

As is shown in Table 4, the energy consumption rises for decreasing pre-cooling temperatures. This is on the one hand based on the higher energy consumption for cooling without the CO_2, on the other hand the heat flux increases at lower temperature due to a higher flow rate. The flow rate increases since the density rises and thus the mass of the CO_2 for the same volume.

At this point an energy efficiency ratio r is introduced which relates the cumulative measured cooling capacity at each of these temperatures for t = 1 min to the total energy consumption of the pre-cooling unit. It is calculated as:

$$r = \frac{\frac{\sum_{0}^{t} P \bullet t}{3600}}{E_{total}}$$

By cumulating the cooling capacity per second, a high accuracy of the power that equals the cooling capacity is ensured. For a comparison to the total energy consumption that is measured over a time frame of t = 1 h, the unit of the cooling capacity has to be transferred to Wh by dividing by 3600. These considerations lead to the following key values shown in Table 5.

As shown in Table 5, the highest energy efficiency with a coefficient of r = 0.50 is found at a pre-cooling temperature of $\vartheta = 16$ °C. However, the highest cooling capacity is achieved at $\vartheta = 14$ °C. The application of a pre-cooling temperature of $\vartheta = 10$ °C leads to the lowest of both values.

As increasing the pressure of the LCO_2 requires compressed air, the energy efficiency needs to be calculated accordingly. For this purpose, the flow rate of the compressed air is measured with a flow rate meter by CS Instruments GmbH & Co. KG over a time span of t = 5 min. This low time frame is selected to reduce the CO_2 consumption at the high LCO_2-flow rates in the setup with the inert gas dosing device DSD 500 by Maximator GmbH and Linde AG. The total air consumption is projected to t = 1 h. According to [32], one cubic meter of compressed air amounts to $E_{air} = 125$ Wh. Together with the electrical energy consumption that is again measured with the power supply measurement device of the type Qualistar+ C. A. 8336 by Chauvin Arnoux, this leads to the following total energy consumption in Table 6.

In the same method as in Table 5, the energy efficiency ratios are calculated. Thus, the cumulative cooling capacity per second is related to the total energy consumption in Table 7.

While an increase in cooling capacity of the LCO_2 is possible by means of pressurization, the overall energy efficiency of the available equipment is subpar. Depending on the process and the means of pressurization, this strategy can be viable, however, the pre-cooling of the LCO_2 is considered the more energy efficient option.

Table 4
Energy consumption of the whole system.

ϑ_{Water} (°C)	ϑ_{CO2} (°C)	ΔT (K)	$\dot{m}$ (kg/h)	$E_{measured}$ (Wh)	E_{total} (Wh)
16	19.2	3.2	3.9	101.0	154.2
14	18.0	4.0	4.1	109.3	179.2
12	15.5	3.5	5.0	111.4	186.0
10	13.5	3.5	5.1	113.7	189.8

Table 5
Calculation of the energy efficiency coefficient r for pre-cooled LCO_2.

ϑ_{Water} (°C)	P (W)	E_{total} (Wh)	r
16	76.8	154.2	0.50
14	79.0	179.2	0.44
12	76.6	186.0	0.41
10	71.7	189.8	0.38

5. Conclusions

In this investigation the effects of CO_2 pre-cooling on the cooling capacity of the cryogenic medium CO_2 for the use in CMQL in machining have been examined. The following results were obtained as part of this investigation:

- The cooling capacity is directly dependent on the distance of the nozzle. In general, a larger distance leads to lower cooling capacities. However, the difference between h = 0.5 cm and h = 2 cm is not substantial. As a realistic application varies in that range, a further specification is not necessary.
- A heat exchanger allows the pre-cooling of the CO_2 in the supply system and pre-cooling of CO_2 enables the re-liquefaction of gaseous CO_2 in the supply line, which may be present due to unfavorable boundary conditions.
- By varying the pre-cooling temperature, the CO_2 condition can be specifically influenced (ϑ, ρ, $\dot{m}$).
- Pre-cooling the CO_2 increases the cooling capacity of CO_2 (compared to no pre-cooling), but there is no linear relationship between the pre-cooling temperature and the cooling capacity. The density influences the flow rate and thus the cooling capacity. However, the impact is reduced after a threshold of $\vartheta = 16$ °C or $\rho = 780$ kg/m^3.
- These results can only be compared to findings in the literature to a limited extent. *Pušavec et al.* state that an increase in flow rate by a factor of two leads to an enhanced cooling capacity. However, the cooling capacity is not doubled as well. This agrees well with the jump in flow rate from an uncooled state to a cooling temperature of

Table 6
Energy calculation for the LCO_2 pressurization.

Pressure (bar)	Required air (m^3/h)	E_{Air} (Wh)	$E_{electrical}$ (Wh)	E_{total} (Wh)
100	7.56	945	85.2	1030.2
150	14.64	1830	87.6	1917.6
200	18.72	2340	88.8	2428.8

Table 7
Calculation of the energy efficiency coefficient r for pressurized LCO_2.

Pressure (bar)	P (W)	E_{total} (Wh)	r
100	114.0	1030.2	0.11
150	118.9	1917.6	0.06
200	122.5	2428.8	0.05

$\vartheta = 14$ °C which also lifts the flow rate from $\dot{m} = 2$ kg/h to $\dot{m} = 4$ kg/h in this study. Again, an improvement in cooling capacity is observed that does not replicate the factor of the flow rate increase. It is assumed that there is an optimum between cooling capacity and CO_2 consumption. [30]

- Since pre-cooling of CO_2 requires additional energy, it is necessary to choose the pre-cooling temperature based on the highest possible efficiency ratio.
- Increasing the pressure is a suitable alternative to stabilize the LCO_2 stream. Furthermore, it improves the cooling capacity compared to the pre-cooling strategy. However, this is connected to a drastic increase in flow rate and thus CO_2 consumption. Furthermore, its energy efficiency with the existing equipment is subpar in comparison to pre-cooling.
- The following limitations and open issues need to be considered. These require further investigation:
- The cooling capacity of the LCO_2 at a pre-cooling temperature of $\vartheta = 10$ °C is unexpectedly low while having a medium density. Even after a detailed analysis of the acquired data, this phenomenon cannot be explained. Further research into this behavior is required.
- Due to the small outlet diameter of the nozzle compared to the surface of the heating plate, it can be assumed that heat conduction takes place in the plate itself and heat dissipation to the environment. This can lead to a non-quantifiable measurement uncertainty, which is constant for all experiments within this investigation. This allows a relative comparison of the measured cooling strategies. However, a quantitative comparison to Pušavec et al. [30] is not possible due to the different system designs.

With regard to the transferability of these results to CMQL, it has already been shown in previous studies that pre-cooled CO_2 increases the atomization of the oils in CMQL and ensures a more homogeneous application of the oil when CMQL is used in machining processes. [7].

CRediT authorship contribution statement

Trixi Meier: Conceptualization, Methodology, Validation, Formal analysis, Investigation, Writing – original draft, Writing – review & editing, Visualization, Supervision, Project administration, Funding acquisition. **Jan Harald Selzam:** Conceptualization, Methodology, Investigation, Writing – original draft, Writing – review & editing. **Andreas Röckelein:** Conceptualization, Methodology, Software, Validation, Formal analysis, Investigation, Writing – original draft, Writing – review & editing, Visualization. **Nico Hanenkamp:** Writing – review & editing, Supervision, Project administration, Funding acquisition.

Declaration of Competing Interest

The authors declare that they have no known competing financial interests or personal relationships that could have appeared to influence the work reported in this paper.

Acknowledgements

This research was partly conducted as part of the sub-project KK5059915KP3 of the collaborative research project ‘coolFlex4sustainability’. The project is funded by the German Federal Ministry for Economic Affairs and Climate Action (BMWK) under the Central Innovation Programme for SMEs (ZIM) on the basis of a resolution of the German Bundestag.

References

[1] Wagner W, et al. D2 Stoffwerte von bedeutenden reinen Fluiden. In: Gesellschaft Verfahrenstechnik VDI, editor. und Chemieingenieurwesen (Hrsg.). VDI-Wärmeatlas. Berlin: Springer-Verlag; 2013. p. 175–356.
[2] Denkena B, et al. Energy efficient machine tools. CIRP Ann 2020;69(2):646–67.
[3] Gross D, et al. Investigation on the productivity of milling Ti6Al4V with cryogenic minimum quantity lubrication. MM Sci J 2019.
[4] Yıldırım Ç, et al. Evaluation of tool wear, surface roughness/topography and chip morphology when machining of Ni-based alloy 625 under MQL, cryogenic cooling and CryoMQL. J Mater Res Technol 2020;9(2):2079–92.
[5] Gross D, Hanenkamp N. Energy efficiency assessment of cryogenic minimum quantity lubrication cooling for milling. Procedia CIRP 2021;98:523–8.
[6] Pfromm PH. Towards sustainable agriculture: fossil-free ammonia. J Renew Sustain Energy 2017;9(3):034702.
[7] Meier Trixi, et al. Influence of carbon dioxide temperature on sprayability and solubility in cryogenic minimum quantity lubrication with bio-based lubricants. Manufacturing Driving Circular Economy. GCSM 2022. Lecture Notes in Mechanical Engineering. Springer; 2023. p. 202–10.
[8] Dillon OW, et al. The effects of temperature on the machining of metals. J Mater Shap Technol 1990;8(1):23–9.
[9] Hong SY, Zhao Z. Thermal aspects, material considerations and cooling strategies in cryogenic machining. Clean Prod Process 1999;1(2):107–16.
[10] Hong SY, Broomer M. Economical and ecological cryogenic machining of AISI 304 austenitic stainless steel. Clean Prod Process 2000;2(3):157–66.
[11] Gross D. Untersuchungen zur kohlenstoffdioxidbasierten kryogenen Minimalmengenschmierung. Dissertation. Erlangen; 2021. https://doi.org/10.25593/978-3-96147-413-4.
[12] Jerold BD, Kumar MP. Machining of AISI 316 stainless steel under carbon-di-oxide cooling. Mater Manuf Process 2012;27(10):1059–65.
[13] Tapoglou N, et al. Investigation of the influence of CO 2 cryogenic coolant application on tool wear. : Procedia CIRP 2017;63:745–9.
[14] Biermann D, et al. Experimental investigation of tool wear and chip formation in cryogenic machining of titanium alloys. : Adv Manuf 2015;3(4):292–9.
[15] Villarrazo N, et al. The effects of lubricooling ecosustainable techniques on tool wear in carbon steel milling. : Mater (Basel, Switz) 2023;16(7).
[16] Grguraš D, et al. Cutting forces and chip morphology in LCO_2 + MQL assisted robotic drilling of Ti6Al4V. : Procedia CIRP 2021;102:299–302.
[17] Sterle L, et al. The effects of liquid-CO_2 cooling, MQL and cutting parameters on drilling performance. : CIRP Ann 2021;70(1):79–82.
[18] Clarens AF, et al. Feasibility of metalworking fluids delivered in supercritical carbon dioxide. J Manuf Process 2006;8(1):47–53.
[19] Wika K, et al. Impact of supercritical carbon dioxide cooling with Minimum Quantity Lubrication on tool wear and surface integrity in the milling of AISI 304L stainless steel. : Wear 2019;426-427:S. 1691–1701.
[20] Khosravi J, et al. High-speed milling of Ti6Al4V under a supercritical CO_2 + MQL hybrid cooling system. : J Manuf Process 2022;82:1–14.
[21] Tapoglou N, et al. Milling of aerospace alloys using supercritical CO_2 assisted machining. : Procedia CIRP 2021;101:370–3.
[22] Stephenson DA, et al. Rough turning Inconel 750 with supercritical CO_2-based minimum quantity lubrication. : J Mater Process Technol 2014;214(3):673–80.
[23] Meier T, et al. Investigation of lubricating oils from renewable resources for cryogenic minimum quantity lubrication. MM Sci J 2021.
[24] Meier T, et al. Comparison of sprayability and solubility of bio-based lubricants with liquid carbon dioxide. MM Sci J 2021.
[25] Iruj M, et al. State-of-the-art hybrid lubrication (Cryo-MQL) supply systems, performance evaluation, and optimization studies in various machining processes. Results Eng 2024;22.
[26] Fusion Coolant Systems. Pure-Cut and Pure-Cut+. Sustainable Cooling and Lubrication for Modern Machining. Available at: ⟨https://www.fusioncoolant.com/solutions/pure-cut⟩ [last visited: 2024–07-22].
[27] Schiller, D., et al. Cool Clean Technologies. Method and apparatus for thermal control within a machining process. WO2012129138A2. Published: 2012–09-27.
[28] HRE Automation. BeCold. Cryogenic lubrication system. Available at: ⟨https://hre.es/en/engineering-solutions/becold-cryogenic-lubrication-system/⟩ [last visited: 2024–07-22].
[29] Knoll Maschinebau. Minimalmengenschmiersystem AerosolMaster 4000 Cryolub. Availabe at: ⟨https://www.knoll-mb.de/produkte/einzelanlagen/mms-systeme/aerosolmastertm-4000-cryolub⟩ [last visited: 2024 07 22].
[30] Pušavec F, et al. Cooling capability of liquid nitrogen and carbon dioxide in cryogenic milling. CIRP Ann - Manuf Technol 2019;68:73–6.
[31] Hanenkamp N, et al. Hybrid supply system for conventional and CO_2/MQL-based cryo-genic cooling. : Procedia CIRP 2018;77.
[32] Dehli M. Energieeffiziente Druckluftechnik. Energieeffizienz in Industrie, Dienstleistung und Gewerbe. Springer Vieweg; 2020.